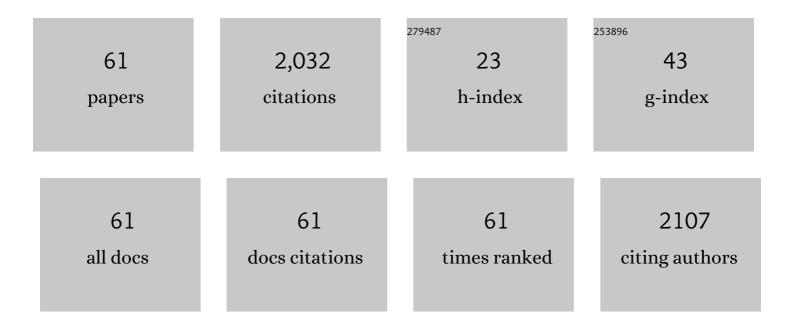
## Zhao Wang

## List of Publications by Year in descending order

Source: https://exaly.com/author-pdf/2764814/publications.pdf Version: 2024-02-01



ZHAO WANC

#	Article	IF	CITATIONS
1	Tuning oxygen vacancies on LaFeO3 perovskite as efficient electrocatalysts for oxygen evolution reaction. Materials Letters, 2022, 309, 131317.	1.3	23
2	In–Ni Intermetallic Compounds Derived from Layered Double Hydroxides as Efficient Catalysts toward the Reverse Water Gas Shift Reaction. ACS Catalysis, 2022, 12, 4026-4036.	5.5	30
3	Facile synthesis of multiphase cobalt–iron spinel with enriched oxygen vacancies as a bifunctional oxygen electrocatalyst. Physical Chemistry Chemical Physics, 2022, 24, 13839-13847.	1.3	7
4	Plasma-assisted defect engineering of N-doped NiCo <sub>2</sub> O <sub>4</sub> for efficient oxygen reduction. Physical Chemistry Chemical Physics, 2021, 23, 6591-6599.	1.3	22
5	Synthesis of oxygen vacancies enriched Cu/ZnO/CeO <sub>2</sub> for CO <sub>2</sub> hydrogenation to methanol. , 2021, 11, 1171-1179.		8
6	Measurement and Correlation of the Solubility and Thermodynamic Properties of Ribavirin(II) in Nine Pure Solvents and (1-Propanol + Water) Binary Solvents. Journal of Chemical & Engineering Data, 2021, 66, 3713-3721.	1.0	6
7	Bi2O3 nanosheets arrays in-situ decorated on carbon cloth for efficient electrochemical reduction of nitrate. Chemosphere, 2021, 278, 130386.	4.2	43
8	NH3•H2O-assisted solvent thermal synthesis of mesoporous spherical NiCo2O4 nanomaterials having rich oxygen vacancies for enhanced activity of CH3OH electrooxidation. Electrochimica Acta, 2021, 390, 138794.	2.6	2
9	ZIF-8 engineered bismuth nanosheet arrays for boosted electrochemical reduction of nitrate. Nanoscale, 2021, 13, 13786-13794.	2.8	9
10	Insight into amoxicillin sodium heterosolvates and non-solvated form: crystal structures, phase transformation behaviors, and desolvation mechanism. CrystEngComm, 2021, 23, 3995-4004.	1.3	2
11	Electron-assisted synthesis of g-C <sub>3</sub> N <sub>4</sub> /MoS <sub>2</sub> composite with dual defects for enhanced visible-light-driven photocatalysis. RSC Advances, 2021, 11, 78-86.	1.7	10
12	Facile Route of Pâ€doped Defectâ€rich Manganeseâ€cobalt Oxide Spinel with Enhanced Oxygen Evolution Reaction Performance. ChemNanoMat, 2020, 6, 1812-1818.	1.5	8
13	Valence, Size, and Shape Control of Gold Nanoparticles Synthesized by Electronâ€Assisted Reduction. Chemistry - an Asian Journal, 2020, 15, 3904-3912.	1.7	3
14	Binary solid solutions of anthracene and carbazole: Thermal properties, structure and crystallization kinetics. Journal of Molecular Liquids, 2020, 309, 112646.	2.3	6
15	Superconducting Nanowire Photon-Number-Resolving Detectors Integrated with Current Reservoirs. Physical Review Applied, 2020, 14, .	1.5	7
16	Enhanced Activity of Cu/ZnO/C Catalysts Prepared by Cold Plasma for CO <sub>2</sub> Hydrogenation to Methanol. Industrial & Engineering Chemistry Research, 2020, 59, 5657-5663.	1.8	20
17	Oxygen Vacancy-Enriched FeOx Nanoparticle Electrocatalyst for the Oxygen Reduction Reaction. Transactions of Tianjin University, 2020, 26, 373-381.	3.3	13
18	An Investigation into the Morphology Evolution of Ethyl Vanillin with the Presence of a Polymer Additive. Crystal Growth and Design, 2020, 20, 1609-1617.	1.4	19

ZHAO WANG

#	Article	IF	CITATIONS
19	Noble Metal-Free TiO2-Coated Carbon Nitride Layers for Enhanced Visible Light-Driven Photocatalysis. Nanomaterials, 2020, 10, 805.	1.9	11
20	Measurement and Correlation of the Solubility of Aspirin in Four Binary Solvent Mixtures from <i>T</i> = 283.15 to 323.15 K. Journal of Chemical & Engineering Data, 2020, 65, 856-868.	1.0	7
21	The mechanism of solvent-mediated desolvation transformation of lenvatinib mesylate from dimethyl sulfoxide solvate to form D. Acta Crystallographica Section B: Structural Science, Crystal Engineering and Materials, 2020, 76, 343-352.	0.5	11
22	A Novel Route to Manufacture 2D Layer MoS2 and g-C3N4 by Atmospheric Plasma with Enhanced Visible-Light-Driven Photocatalysis. Nanomaterials, 2019, 9, 1139.	1.9	19
23	Plasmon Based Doubleâ€Layer Hydrogel Device for a Highly Efficient Solar Vapor Generation. Advanced Functional Materials, 2019, 29, 1901312.	7.8	136
24	Novel Technology for Separation of Binary Eutectic-Forming Mixture by Cocrystallization into Different Sizes Combined with Particle Size Fraction. Industrial & Engineering Chemistry Research, 2019, 58, 8800-8809.	1.8	6
25	Thermodynamic mechanism of selective cocrystallization explored by MD simulation and phase diagram analysis. AICHE Journal, 2019, 65, e16570.	1.8	33
26	Electron reduction for the preparation of rGO with high electrochemical activity. Catalysis Today, 2019, 337, 63-68.	2.2	22
27	Solubility and mixing thermodynamic properties of (2,4,6-trimethylbenzoyl) diphenylphosphine oxide in pure and binary solvents. Fluid Phase Equilibria, 2018, 461, 57-69.	1.4	20
28	Catalyst Preparation with Plasmas: How Does It Work?. ACS Catalysis, 2018, 8, 2093-2110.	5.5	323
29	Enhanced hydrogen production from water on Pt/g-C3N4 by room temperature electron reduction. Materials Research Bulletin, 2018, 104, 1-5.	2.7	41
30	Effect of TS-1 Treatment by Mixed Alkaline on Propylene Epoxidation. Transactions of Tianjin University, 2018, 24, 25-31.	3.3	8
31	Determination and Correlation of the Solubility of Acetylpyrazine in Pure Solvents and Binary Solvent Mixtures. Journal of Solution Chemistry, 2018, 47, 950-973.	0.6	3
32	Multivalent manganese oxides with high electrocatalytic activity for oxygen reduction reaction. Frontiers of Chemical Science and Engineering, 2018, 12, 790-797.	2.3	17
33	Simultaneous Effects of Multiple Factors on Solution-Mediated Phase Transformation: A Case of Spironolactone Forms. Organic Process Research and Development, 2018, 22, 836-845.	1.3	8
34	Thermodynamic properties of metamizol monohydrate in pure and binary solvents at temperatures from (283.15 to 313.15) K. Chinese Journal of Chemical Engineering, 2017, 25, 1481-1491.	1.7	5
35	Performance of Methanol-to-Olefins Catalytic Reactions by the Addition of PEG in the Synthesis of SAPO-34. Transactions of Tianjin University, 2017, 23, 501-510.	3.3	7
36	Determination of metastable zone and induction time of analgin for cooling crystallization. Chinese Journal of Chemical Engineering, 2017, 25, 313-318.	1.7	25

ZHAO WANG

#	Article	IF	CITATIONS
37	Preparation and Dehydration Kinetics of Complex Sulfadiazine Calcium Hydrate with Both Channel-Type and Coordinated Water. Organic Process Research and Development, 2016, 20, 780-785.	1.3	6
38	From Jellylike Phase to Crystal: Effects of Solvent on Self-Assembly of Cefotaxime Sodium. Industrial & Engineering Chemistry Research, 2016, 55, 3075-3083.	1.8	18
39	Highly efficient, stable and controllable multi-core, rattle-type Ag@SiO <sub>2</sub> catalyst for the reduction of 4-nitrophenol. RSC Advances, 2016, 6, 95263-95272.	1.7	12
40	Process Design for Antisolvent Crystallization of Erythromycin Ethylsuccinate in Oiling-out System. Industrial & Engineering Chemistry Research, 2016, 55, 7484-7492.	1.8	27
41	Antisolvent Crystallization of Erythromycin Ethylsuccinate in the Presence of Liquid–Liquid Phase Separation. Industrial & Engineering Chemistry Research, 2016, 55, 766-776.	1.8	21
42	Steam reforming of methane over Ni/SiO2 catalyst with enhanced coke resistance at low steam to methane ratio. Catalysis Today, 2015, 256, 130-136.	2.2	109
43	A simple plasma reduction for synthesis of Au and Pd nanoparticles at room temperature. Chinese Journal of Chemical Engineering, 2015, 23, 1060-1063.	1.7	9
44	Formation of Solid Solution and Ternary Phase Diagrams of Anthracene and Phenanthrene in Different Organic Solvents. Journal of Chemical & Engineering Data, 2015, 60, 1401-1407.	1.0	18
45	Mechanism of template removal for the synthesis of molecular sieves using dielectric barrier discharge. Catalysis Today, 2015, 256, 137-141.	2.2	30
46	Spherulitic Crystallization of <scp>L</scp> -Tryptophan: Characterization, Growth Kinetics, and Mechanism. Crystal Growth and Design, 2015, 15, 5124-5132.	1.4	34
47	Solubility of androstenedione in lower alcohols. Fluid Phase Equilibria, 2014, 363, 86-96.	1.4	45
48	Solubility of Cefotaxime Sodium in Ethanol + Water Mixtures under Acetic Acid Conditions. Journal of Chemical & Engineering Data, 2014, 59, 1865-1871.	1.0	5
49	Experimental Determination and Computational Prediction of Androstenedione Solubility in Alcohol + Water Mixtures. Industrial & Engineering Chemistry Research, 2014, 53, 11538-11549.	1.8	28
50	Lattice instability of V2AlC at high pressure. Science China: Physics, Mechanics and Astronomy, 2013, 56, 916-924.	2.0	13
51	Determination of the Solubility, Dissolution Enthalpy, and Entropy of Pioglitazone Hydrochloride (Form II) in Different Pure Solvents. Industrial & Engineering Chemistry Research, 2013, 52, 3036-3041.	1.8	38
52	Correlation of solubility of pioglitazone hydrochloride in different binary solvents. Fluid Phase Equilibria, 2013, 352, 14-21.	1.4	28
53	Methanation over Ni/SiO2: Effect of the catalyst preparation methodologies. International Journal of Hydrogen Energy, 2013, 38, 2283-2291.	3.8	172
54	Solid–Liquid Phase Equilibrium and Mixing Properties of Cloxacillin Benzathine in Pure and Mixed Solvents. Industrial & Engineering Chemistry Research, 2013, 52, 3019-3026.	1.8	107

ZHAO WANG

#	Article	IF	CITATIONS
55	Correlation of Solubility and Prediction of the Mixing Properties of Ginsenoside Compound K in Various Solvents. Industrial & Engineering Chemistry Research, 2012, 51, 8141-8148.	1.8	59
56	Correlation of Solubility and Prediction of the Mixing Properties of Capsaicin in Different Pure Solvents. Industrial & Engineering Chemistry Research, 2012, 51, 2808-2813.	1.8	87
57	Preparation of highly efficient Au/C catalysts for glucose oxidation via novel plasma reduction. Catalysis Communications, 2012, 25, 92-95.	1.6	24
58	Enhanced Hydrogen Spillover on Carbon Surfaces Modified by Oxygen Plasma. Journal of Physical Chemistry C, 2010, 114, 1601-1609.	1.5	71
59	Enhanced Hydrogen Storage on Pt-Doped Carbon by Plasma Reduction. Journal of Physical Chemistry C, 2010, 114, 5956-5963.	1.5	48
60	Size control of carbon black-supported platinum nanoparticles via novel plasma reduction. Catalysis Communications, 2009, 10, 959-962.	1.6	23
61	Hydrogen Storage on Carbon Doped with Platinum Nanoparticles Using Plasma Reduction. Industrial & Engineering Chemistry Research, 2007, 46, 8277-8281.	1.8	60